

The Significance of Sclera Colour and Eye Movement Patterns in the Uncanny Valley

Effect: An Eye-Tracking Study

Jamy Lee Marie Borninkhof

Bachelor Thesis

Faculty of Behavioural, Management and Social Sciences (BMS),

University of Twente

Human Factors and Engineering Psychology

First Supervisor: Martin Schmettow

Second Supervisor: (Nienke Bierhuizen)/Marlise Westerhof

04/07/2022

Table of Contents

Abstract	2
Introduction	3
The Uncanny Valley Effect.....	3
Evolutionary Roots of the Uncanny Valley Effect.....	5
The Influence of Perceptual Mismatch.....	6
Face Processing.....	6
Holistic Face Processing or Analytical Face Processing.....	8
The Link between Eyes, Sclera Colour, and the Uncanny Valley Effect.....	9
In this Study.....	10
Methods	11
Participants.....	11
Materials.....	11
Likeability Scale.....	15
Procedure.....	15
Data Analysis.....	17
Results	20
Uncanniness Ratings.....	20
Visual Exploration Patterns.....	23
Total Distance Travelled and Number of Visits.....	23
Dwell Time per AOI.....	25
Discussion	28
Dark Sclera on Human Faces in Video Games.....	29
Evolution and Dark Sclerae on Human Skulls.....	29
Face Processing and Attention.....	30
The YET0-Eye Tracker.....	32
Implications for Future Research.....	33
Conclusion	33
References	34
Appendix	43
A: Stimulus Set.....	43
B: Participant Forms.....	46
C: R Code.....	49

Abstract

This study is aimed at determining the role of sclera colour and eye movement patterns in the Uncanny Valley Effect (UVE). The UVE describes a phenomenon in which a character's likeability is dependent on their human likeness. Typically, the more human-like a character is the more likeable they are. However, this effect predicts a sharp drop in likeability when a character is somewhat but not quite human-like. A previous study has made unexpected findings suggesting that white mismatching sclera on ape-like faces may be correlated with this drop in likeability. Therefore, an eye-tracking study was employed, in which a sample of 30 participants was presented with 16 pictures of ape and human faces. One-half of this stimulus set consists of original images, while the other half had been manipulated to have the opposite sclera colour. After the presentation of the stimulus set, uncanniness ratings were collected for each individual picture. Results demonstrated differences in responses to incongruent faces compared to congruent faces. Unexpectedly, the findings show additional differences in uncanniness ratings and eye movement patterns between different types of incongruences. Namely, human-like skulls with ape-like dark sclera were perceived as uncannier and elicited less dwell time on central facial features and a smaller number of total visits than all other conditions.

Introduction

In response to the global call for social distancing, online social networking systems have become increasingly popular. In an attempt to tackle subsequent technological exhaustion, several companies have employed strategies to make such systems more exciting through innovation (Giuseppe et al., 2020; Wiederhold, 2022). For example, electronic-game companies such as Epic Games and Roblox have begun holding immersive virtual live concerts (Bobrowsky, 2021). Further, the big technology corporation Microsoft is developing the software Microsoft Mesh, which has multi-user mixed reality functions (Bobrowsky, 2021). In such applications, users can use digital avatars to meet in online virtual spaces in real-time.

In such systems, the designs of virtual avatars may significantly influence social interaction. For instance, Nowak and Rauh (2008) have found that impressions of virtual avatars skew the perception of their users' credibility. In fact, this perception of trustworthiness may be crucial in users' decisions to accept or reject friend requests (Shin et al., 2019). Therefore, there is a need for designing likeable avatars. One relevant factor in creating an appealing avatar is human likeness, which has generally been linked with higher rates of trustworthiness and likeability (Nowak et al., 2009; Nowak & Rauh, 2005; Walther & Bunz, 2005). However, some of the following research suggests an effect that implies that certain levels of human likeness can negatively affect the degree to which users perceive virtual avatars as likeable and trustworthy.

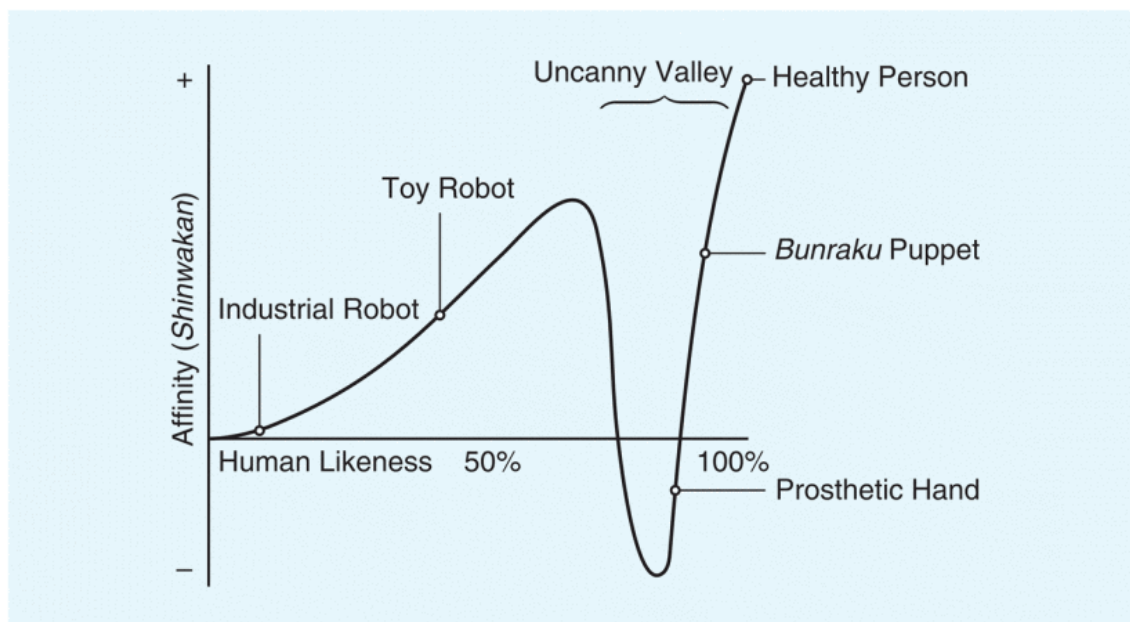
The Uncanny Valley Effect

The so-called Uncanny Valley Effect (UVE) describes the eeriness experienced in response to looking at an almost-yet-not-completely human-like character. This effect was first proposed by Mori during his research on robotics in the 1970s (Mori et al., 2012).

According to the UVE, a character's human likeness increases observers' affinity up to a certain point (see Figure 1). Approximately at a moderate-to-strong human likeness, there is a sharp drop in affection that is commonly accompanied by an uncomfortable feeling. This drop is commonly referred to as the uncanny valley. As depicted by the graph in Figure 1, the uncanny valley is followed by a sharp increase in affinity once the depicted character is almost indistinguishable from humans. This poses an extraordinary challenge of balancing human-like features in the design of virtual avatars.

Figure 1

The Uncanny Valley Effect: The Relationship between an Object's Human Likeness and Affinity



Note. [Bunraku puppets are used by groups of three puppeteers in traditional Japanese musical theatres. These one-metre-big puppets wear detailed costumes.] From “The Uncanny Valley [From the Field]” by M. Mori et al.. 2012, *Robotics & Automation Magazine*, 19(2), p. 99. Copyright [2012] by IEEE.

Consequently, follow-up research has become more popular in the last couple of decades. For instance, insights about the UVE have been gained through studies on uncanny characters in computer animation commonly used in the entertainment industry (e.g., Burleigh et al., 2013; MacDorman et al., 2009). Research on the UVE has expanded far beyond robotics and computer-generated characters, inspiring studies in fields such as neuroimaging and child psychology (e.g., Cheetham et al., 2011; Matsuda, 2012; Urgen et al., 2018). More recently, Marthur and Reichling (2016) have successfully solidified the empirical evidence on the existence of the UVE, as well as its universality across individuals. Further suggesting the robustness of this effect, Alvarez Perez et al.'s (2020) research on the UVE has shown that increased prior experience with robots does not seem to affect the characteristic drop in affinity. In brief, the UVE is a relatively robust effect that is relevant across various fields of study. Because of this, this study seeks to further investigate the specific causes for the UVE. To explore this, the origins of the UVE need to be taken into account.

Evolutionary Roots of the Uncanny Valley Effect

The universality of the UVE suggests the idea that its origins can be traced back to evolutionary rather than culturally dependent factors. There are multiple findings that align with the idea of the UVE's possible evolutionary origins. For instance, there have been indications that the UVE may be experienced by macaque monkeys (Steckenfinger & Ghazanfa, 2009). Thus, the UVE might be a consequence of human phylogenesis. The idea of an evolutionary origin is further supported by a study conducted by Haeske and Schmettow (2016) who found that faces could be identified through a fast-processing system rather than slow systems that would require deliberate evaluation. Hence, early visual neural systems are involved, which date back to older evolutionary roots.

Possible evolutionary explanations for the UVE revolve around threat deception and self-preservation (Mori et al., 2012). In an attempt to preserve oneself, there were two major threats avoidable through quick face processing. To begin, sensitivity to human likeness is beneficial as an indicator to avoid harmful genetic abnormalities or diseases (MacDorman et al., 2009). This becomes increasingly relevant for humans as genetic likeness rises, which in turn increases the risk for the spreading of pathogens (MacDorman et al., 2009). Furthermore, the UVE could be linked to mechanisms revolving around deception detection as acts of deception are usually performed with negative intentions (Moore, 2012). Therefore, the UVE may serve an evolutionary purpose as part of a survival mechanism.

The Influence of Perceptual Mismatch

Nevertheless, human likeness may not fully account for the UVE. Kätsyri et al. (2015) reviewed literature on likely origins for the UVE. These researchers concluded that evidence supports that the characteristic drop in affinity is often attributed to a mismatch between human-like and human-unlike features (Kätsyri et al., 2015). For instance, Kätsyri et al. (2015) describe that one may feel that a character looks uncanny if they have human eyes on a non-human face. In brief, faces may be perceived as uncanny if they consist of a mismatch of human-like and human-unlike features. Consequently, it is plausible to assume that there might be a difference in the way incongruent faces are processed compared to congruent faces.

Face Processing

While evidence has been collected for the universality and origins of the UVE, little research has been done on which mismatching features are most influential in causing a human-like character to be perceived as uncanny. Most studies in this area have focused on

the face as a whole, which represents a core factor in human interaction (Yu, 2011). This is in part due to the fact that faces are naturally salient (de Gelder et al., 2006). In addition to this, faces are attention-grabbing as they are associated with speech and other complex perceptual information. Through face perception, individuals can gain information about another's thoughts and feelings, which greatly influences how people interact with each other (Tanaka & Sung, 2013). Consequently, if individuals experience a human-like character's design as uncanny it is most likely due to incongruent facial features as opposed to other bodily characteristics.

Evidence suggests that the processing of human-like faces has evolved to be distinct from that of non-human faces and objects. This can be observed early on in infancy, during which infants clearly prefer face-like patterns such as three dots arranged in a triangular orientation compared to other patterns (Goren et al., 1975; Valenza et al., 1996). This preference may be caused by pre-existing brain structures specialised in face perception, such as the fusiform gyrus (Haxby et al., 2000; Kanwisher & Yovel, 2006; McCarthy et al. 1997). In turn, these processes aid in the further development of these relevant neural structures (de Haan et al., 2002). Possibly as a consequence of this, three-month-old infants start to form an inner representation of the facial area (de Haan et al., 2002). This expresses itself in a preference of human-like over monkey-like faces (di Giorgio et al., 2013). Therefore, humans develop an internal facial model from an early age on. Based on this model, some faces are experienced as more or less typical or atypical. It is likely because of this, that face processing may be the most advanced perceptual ability allowing humans to evaluate faces within merely a few milliseconds (Haxby et al., 2002; Landwehr, et al., 2011). This internalised face model lays the groundwork for the special way in which humans process faces.

Holistic Face Processing or Analytical Face Processing

In general, literature distinguishes between two ways of human face processing depending on whether human or non-human. Since humans have an internal face model, they are able to perceive conspecific faces holistically (Farah et al., 1998; Richler & Gauthier, 2014). It is believed that this type of processing facilitates the ability to identify individuals, which is a necessary component of human interaction (Farah et al., 1998; Richler & Gauthier, 2014). However, when human faces are not in typical configurations, for example when they are inverted, they cannot be processed holistically (Dahl et al., 2014). Instead, atypically configured faces are processed much like non-human faces, such as those of monkeys (Mega & Volz, 2017). This processing approach is more analytical as it is characterised by an increased amount of eye fixations and time (Dahl et al., 2014; Mega & Volz). Therefore, human likeness plays a key role in whether faces are processed holistically.

Holistic face processing has been supported by two types of experiments. First, Tanaka and Farah (1993) used the so-called part-whole task, in which participants were instructed to recognise face parts they had seen in advance. Recognition was better for those participants who had seen these face parts in the context of a whole face instead of as separate parts. Second, researchers have found indications for holistic face processing based on results of the composite face task (Le Grand et al., 2004; Young et al., 1987). During this task, two inconsistent halves of a face were presented to participants. Typically, recognition performance improves when these halves are misaligned rather than joint. In addition to this, it has been recorded that patients with impaired facial recognition seem to display defective holistic processing in this task (Avidan et al., 2011; Le Grand et al., 2006). Nevertheless, there are some facial features humans pay more attention to than others.

The Link between Eyes, Sclera Colour, and the Uncanny Valley Effect

The central role of human eyes and eye movements has been supported by evidence from eye-tracking studies aimed at exploring face processing. Bagepally (2015) concluded that people have the tendency to look at the upper face half close to the eyes when initially shown a face. Iskra and Tomc's (2016) findings confirmed that the primary area of fixations is around the eyes. Significantly more rarely, participants would also fixate on the general mouth area (Iskra & Tomc, 2016). However, since face processing is holistic, it is reasonable to assume that if the eyes would not fit the rest of a face, there may be more exploration in an attempt to find consistency between eyes and other facial features such as the general mouth area.

Such findings can be explained by considering that eyes and eye movements are especially important in human interaction. Commonly, the eye region is believed to be the location of the self (Starmans & Bloom, 2012). Because of this, human-like eyes are one of the most decisive factors in how trustworthy humans believe characters to be (e.g., Kaisler & Leder, 2016; Landwehr et al., 2011). Some influential characteristics of the eyes include overall shape, colour and size (Santos & Young, 2011; Todorov et al., 2008). More specifically, Geue and Schmettow (2021) found the uniquely white sclerae of human eyes to be a common feature of stimuli perceived as uncanny in their study. This may be traced back to how human eyes evolved to have white sclerae in contrast with other primates (Kobayashi & Kohshima, 1997; Kobayashi & Kohshima, 2001). There are various reasons why the development of white sclerae may have been beneficial.

Tomasello et al. (2007) believe that one likely origin may fall in line with their cooperative eye hypothesis. Because of the high contrast between the white sclerae, iris and pupil, it is easy for humans to perceive and follow each other's gaze (Kobayashi & Kohshima, 2008). According to Tomasello et al. (2007), this serves as the basis of an advantageous

cooperation strategy by allowing humans to communicate non-verbally more easily. Another potential benefit of white sclerae may be the ability to gauge someone's age and health, and to therefore, determine how attractive potential mates are (Provine et al., 2013; Tomasello et al., 2007). As a result, the UVE is most likely to occur in responses to non-human faces with white sclerae or human faces without white sclerae.

In this Study

In conclusion, we believe that a human-like character's eyes will serve as a reference point while other facial features play a secondary role. Since the UVE occurs when such features are incongruent, we reckon that people's fixations would shift back and forth between a character's eyes and all other relevant facial features, thereby demonstrating an increased number of fixations and gaze distance travelled compared to congruent faces. Additionally, we believe that sclera colour that is incongruent with the rest of a face is a driving factor in whether this face is perceived to be uncanny. Therefore, we pose the following hypotheses about sclera colour and how gaze and fixation patterns differ in response to incongruent faces relative to congruent faces:

- Relative to congruent faces, mismatching sclera colour with the rest of a face predicts that a face is perceived to be uncannier.
- The number of visits is higher in response to incongruent faces relative to congruent faces.
- Gazes travel larger total distances in response to incongruent faces relative to congruent faces.
- There is a larger dwell time per area of interest for facial features other than the eyes in response to incongruent faces compared to congruent faces.

Methods

To investigate these hypotheses, this eye-tracking study was conducted. Participants were exposed to primate faces with different levels of uncanniness and partially manipulated sclera colour.

Participants

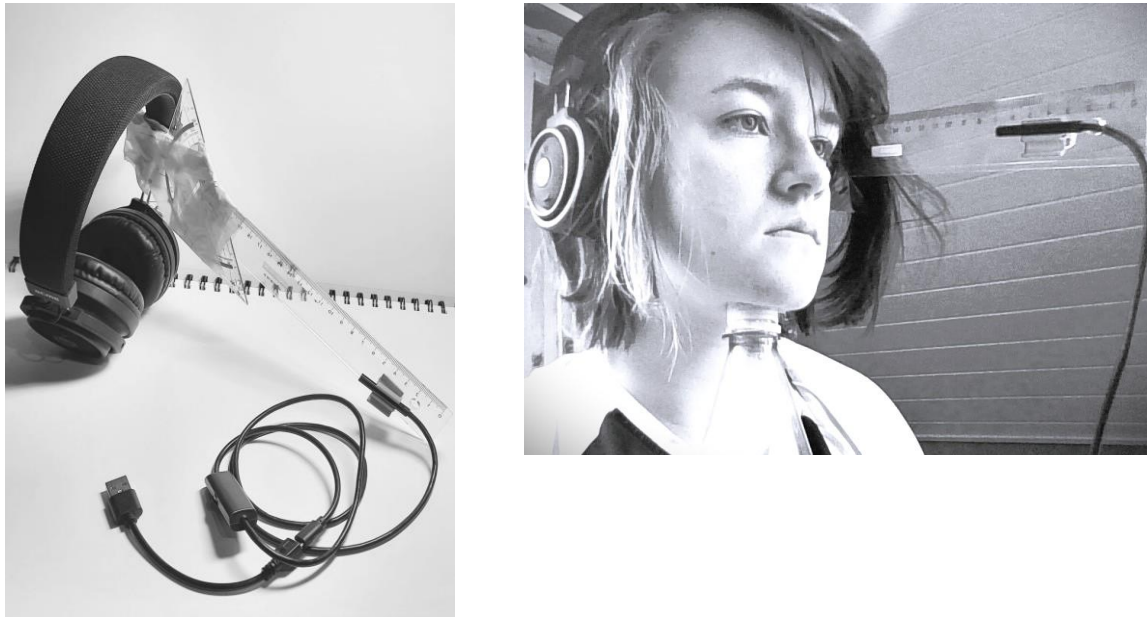
The recruitment of participants was conducted by means of personally contacting fellow students and other people acquainted with the researchers. In total, 30 participants took part in this study. Demographic data were not collected due to their irrelevance in examining the hypotheses of this study. Further, this decision was made to protect participants' privacy rights. This study was approved by the Ethics Committee of the University of Twente's BMS faculty.

Materials

YETO-Eye Tracker

For this study, we used the *YETO-eye tracker* (Schmettow & Brandl, 2021). This device consists of a 5.5-diameter-USB-LED-endoscope-camera with a 240x480 resolution and 30Hz sample rate that is fixed to a 30-cm-long ruler via a custom 3D-printed clip (see Figure 2). This ruler was mounted onto headphones so as to stay in place throughout the experiment while simultaneously being comfortable for participants to wear. For additional stability, a set square was used to balance out the weight distribution of this head mount.

The *YETO-eye tracker* runs on *YETA1*, a software developed in *Python* by members of the University of Twente. On the basis of the *YETO-eye tracker's* recordings, this programme calculates and records participants' eyeball coordinates and time stamps, which can be used for further analyses.

Figure 2*YET0-Eye Tracker with Head Mount****Stimulus Set***

The selected stimuli are a subset of those used by Geue and Schmettow (2021). The original stimulus set used by these researchers contained a total of 90 pictures, out of which 11 were robot faces and 89 were primate faces. These pictures were chosen with the aim to achieve a vast array of human likeness levels. To do so, these researchers had obtained these pictures and permission for their usage from John Gurche's hominin photographs, and from the two open-access databases PrimFace and the Global Biodiversity Information Facility (Global Biodiversity Information Facility, n.d.; Gurche, n.d.; RIKEN Center for Brain Science, 2018). These scholar's aim was to determine eeriness scores and their relation to human likeness levels to map each stimulus' position on the UV curve (Geue & Schmettow, 2021). To do so, Geue and Schmettow (2021) determined the stimuli's human likeness levels by averaging scores given by four different observers. Subsequently, stimuli with low inter-

rater reliability were excluded from their study. To determine uncanniness of stimuli, Geue and Schmettow (2021) gathered data with two visual analogue scales (VAS). These included Ho and MacDorman's (2017) eeriness index 'spine-tingling' subscale as well as Marthur and Reichling's (2016) one-item VAS (Geue & Schmettow, 2021).

The subset we chose consists of eleven photographs of ape and monkey faces previously used by Geue and Schmettow (2021). Two out of these pictures were used as dummies so that participants could get used to the experiment's procedure. The remaining nine stimuli were chosen based on three different rating-based positions on the UV curve. Hence, we picked three stimuli positioned at the shoulder of the UV curve, four at the lowest point of the valley and two at the upwards slope. To do so, we determined the human-likeness cut-off values of these researchers' UV curve data to be: 0 to 50 for the shoulder, 50 to 80 for the valley, and 80 to 100 for the upwards slope. All nine stimuli depict faces from a frontal or a three-quarter view angle so that both eyes could be seen.

Sclera Manipulation. In their study, Geue and Schmettow (2021) hypothesised the central role of sclera colour in the UVE. Because of this, we manipulated the stimuli set in the following way: We prepared two variations of each face in the stimuli set. Sclerae that had originally been white were turned dark, while those that had been dark were turned white (see examples in Figure 3). This was done in three steps with basic photo-editing tools in a graphics software called *Clip Studio Paint*. First, on a new layer, we painted either black or white on top of the sclerae on the original photographs. Second, we lowered the new layer's opacity by 10% to ensure that shadows were still visible. Lastly, we blurred the edges to blend in with the rest of the image. Consequently, half of the stimuli's skull shapes and sclerae were congruent, while the other half was incongruent.

Data Exclusion. Due to a mistake made during this manipulation procedure, one stimulus and its incorrectly manipulated version had to be excluded from the data analysis. This face had black sclerae and an ape-like skull and had been previously rated to be positioned at the shoulder of the UV curve (see final stimulus set in Appendix A).

Figure 3

Sclera Manipulation Examples



Before sclera manipulation.



After sclera manipulation.



Before sclera manipulation



After sclera manipulation.

Face Coding. Four areas of interest (AOIs) were defined in terms of rectangles encompassing certain facial features (see example in Figure 4). AOIs were defined as

the general eye area, the nose, the mouth, and ‘outside’ for all other remaining areas of the face.

Figure 4

Four AOIs: Face Coding Example



Single-Item Likeability Scale

Participants filled in the visual analogue scale adopted from Marthur and Reichling (2016) by Geue and Schmettow (2021) to determine how uncanny participants rated each stimulus to be. In response to the statement ‘To me, this face seems...’, participants could pick a number between -100 to 100 on a single-item likeability scale. Low values are associated with the words ‘unpleasant’, ‘unfriendly’ and ‘creepy’ and higher values stand for ‘pleasant’ and ‘friendly’. Being a continuous scale, more psychometrically accurate data is to be expected in comparison to ordinal Likert scales (Marthur & Reichling, 2016; Reips & Funke, 2008).

Procedure

At the start of the session, the participant sits down at a desk in front of the laptop in a bright room. To ensure the room is sufficiently well-lit to allow for a clear image of the

participants' eyes, a desk lamp is turned on. Then, the participant is informed about the length, possible risks, their rights, and the contents of the experiment. Following this, the participant receives the information sheet and signs their informed consent form (see Appendix B). If the participant wears glasses, they are asked to take them off to prevent measurement errors that may occur as a consequence of light reflections.

To begin with, the participant puts on the *YETO-eye tracker* that is connected to the researcher's laptop. According to the researcher's instructions, the participant assumes a straight posture and rests their head on either a paper towel roll, foam roller or a full water bottle fixed to the table to assure that they do not move their head during the experiment to avoid measuring error. This is necessary as the eye tracker used in this study does not track head movements. Then, the researcher begins to run the eye-tracking programme, after which participants calibrate the programme to properly record their eye movements. To do so, participants look at a coloured dot on the screen while pushing a key. Whenever the participant pushes this key, the coloured dot will appear in a different position on the screen for the participant to look at. After twelve repetitions, a cross will appear on the screen that ideally matches the position of the screen the participant is looking at. If the researcher and participant deem the calibration to be erroneous, the participant recalibrates the eye tracker by repeating this process until a proper calibration is reached.

After a successful calibration, the first two dummy pictures will be displayed so as to allow the participant to get used to the process of keeping as still as possible while focusing on the faces presented to them. Following each face's presentation, there is a brief eye-tracking recalibration shortly before the presentation of each new stimulus. The participant does this by looking at merely one coloured dot in the middle of the screen while pressing a key. In total, the participant looks at 20 pictures of faces presented to him or her on the laptop

screen for five seconds each. Afterwards, the participant takes off the *YETO*-eye tracker while the eye-tracking data is saved.

Subsequently, the researcher opens a slideshow with the eye-tracking experiment's stimuli. The participant uses the continuous on-paper rating scale to evaluate each stimulus based on how creepy, unfriendly, friendly, and pleasant they are. There is no time limit for the participant to rate each stimulus and they may advance to subsequent pictures by pressing a key. Afterwards, the participant is thanked and is informed that they can ask any further questions they may have about the experiment. All in all, this study takes approximately 5 minutes.

Data Analysis

Aggregating Consecutive Saccades into Fixations

In order to transform the coordinates contained in raw eye-tracking data into measures for gaze duration and saccade distance, an algorithm was developed. First, as suggested by Salvucci & Goldberg (2000), a threshold value of 50 pixels was compared to every consecutive movement distance to discriminate between saccades and fixations. Afterwards, the Euclidean distance between pairs of successive measurements was determined.

If a distance measure was larger than or equal to 50 pixels it was counted as a saccade, whereas it was determined to be a fixation candidate if a particular distance fell below this threshold. Afterwards, consecutive distances were joined into either a saccade cluster or a candidate fixation group depending on their group allocation.

To avoid the recording of overly brief fixations, a smoothing process was used. In line with Hooge et al. (2022), if fixation candidates were longer than 60ms they were counted as final fixations. If these candidates were shorter than 60ms they were counted as saccades and, therefore, grouped in with directly preceding and successive saccades.

Transforming Raw Eye-Tracking Data into Measures

The transformation of raw eye-tracking data into measures for gaze duration and saccade distance was accomplished in the following ways. To begin with, saccade distance was determined by calculating the Euclidean distance. Second, the duration of fixations and durations was computed by subtracting their starting measures from their ending time measures. Additionally, average coordinates were calculated for each fixation to describe their position.

Eye-Tracking Measures

There are three ways in which the transformed eye-tracking data was interpreted in further analyses. To determine whether there was more visual exploration in response to uncanny faces, two different measures were used. To begin with, the total distance travelled was computed for each participant. This was done by adding up all individual saccade distances per stimulus. Then, the number of visits was calculated by adding up all visits per stimuli. Lastly, the total fixation duration per AOI was calculated to determine the dwell time per AOI.

Statistical Modelling

In this study, a two (i.e., sclera colour) by two (i.e., skull type) within-subjects design was used. To begin with, this design was simplified into a two-factor model. For this, the predictor variable congruence was used. This variable represents whether a stimulus' sclerae (white human-like vs. dark ape-like) matched its face shape (human-like vs. ape-like). Because of this, congruence consisted of the levels 'congruent' and 'incongruent'. Additionally, the more complex model using both sclerae, skull and the interaction of these

two variables was employed as a predictor to determine whether there are differences between different variations of congruence.

Based on these two designs, multilevel factorial models with random participant effects were created in the statistics software *R* (see R Code in Appendix C). These random effects were chosen as observations are not independent of one another in repeated measures designs. Distribution types were chosen in accordance with Schmettow's (2021) recommendations. More specifically, a beta regression was used to analyse the effect of the predictor variables on the uncanniness ratings. To conduct this regression, the rating scale ranging from -100 to 100 was transformed into a scale from 0 to 1. This was done by adding the value 101 to all rating scores. Afterwards, these scores were divided by 202, finalising the scale transformation. Further, a negative binomial regression was calculated for the outcome variable number of visits. Then, a Gamma regression was employed on the total distance travelled because of the existence of a zero point and the lack of an upper bound.

Lastly, because of the complexity and high volume of data, a population-level model was calculated for the outcome variable dwell time per AOI instead of a multi-factorial design. For this, a Gamma distribution was used for the outcome variable dwell time per AOI.

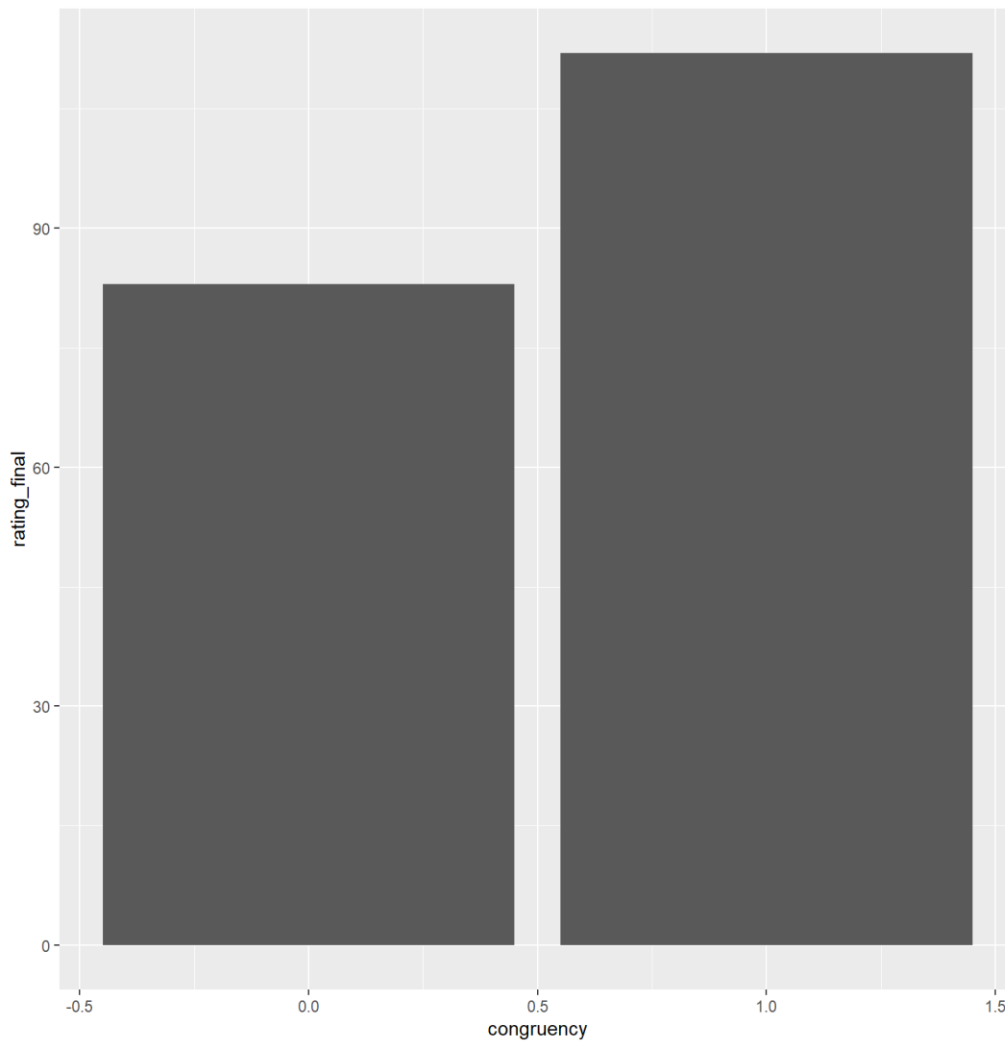
Results

This section serves to find out whether an incongruence between skull shape and sclera colour contributes to how uncanny a face is rated to be. Further, this section is meant to investigate the potential differences in visual exploration patterns arising from congruence and different combinations of human and ape-like skulls and sclerae. To do so, the variables congruence, as well as sclerae by skull, were used as predictors for the outcome variables in the following order: uncanniness ratings, the number of visits, total distance travelled, and dwell time per AOI. Multilevel regression models with random participant effects were used for all of these outcome variables excluding dwell time per AOI.

Uncanniness Ratings

To begin with, it was hypothesised that incongruent stimuli would be perceived to be uncannier than those that are congruent. Therefore, it was expected that there is a positive effect of congruence on uncanniness ratings. To test this, mean values were calculated and displayed in a bar chart (see Figure 5). It was found that the mean of the congruent condition was higher than that of the incongruent condition, which is in concurrence with this study's hypothesis.

To estimate the effect sizes, a multilevel beta regression with a random participant effect was run (see Table 1). However, the confidence interval for this effect displays a range from negative to positive values, suggesting uncertainty about this effect. Within the boundaries of a 95% confidence interval (CI), the random effect is estimated to be between 0.02 and 0.25. This points to a moderately large amount of variation between participants. This model's fixed effect coefficient indicates a small positive effect of congruence on uncanniness ratings.

Figure 5*Bar Chart: Mean Uncanniness Ratings by Congruence***Table 1***Multilevel beta Regression Coefficients of Uncanniness Ratings by Congruence*

	Fixed	CI-95%	CI-95%	Random	CI-95%	CI-95%
effect	estimate	Lower	Upper	Factor	Lower	Upper
		Boundary	Boundary		Boundary	Bound
Intercept (incongruent)	-0.23	-0.39	-0.07	0.23	0.08	0.41

Congruence	0.15	-0.03	0.33	0.1	0.02	0.25
------------	------	-------	------	-----	------	------

To determine whether the type of congruence and incongruence influence effect estimates, skull and sclerae were used as predictor variables. Therefore, a multilevel beta regression of the model rating score by sclerae and skull with a random participant effect was calculated (see Table 2). There was considerable variation among participants, with random effects ranging from 0.19 to 0.38. Overall, there were conditional negative effect estimates for human eyes and for human sclerae, while there were conditional positive effects for congruent stimuli. In concurrence with the hypothesis in this study, this implies that congruent faces were rated to be less uncanny than incongruent faces. Notably, the effect was bigger for ape-like sclerae in human skulls rather than human sclerae on ape-like faces. Out of the congruent stimuli, congruent human faces were rated to be uncannier than those of apes. As a consequence of the differences in effects between different types of incongruences and congruence, it was demonstrated that sclerae and skull models hold more informative value. Therefore, models of congruence by outcome variables were omitted from further analyses.

Table 2

Multilevel beta Regression Coefficients of Uncanniness Ratings by Sclerae and Skull

	Fixed Effect Estimate	CI-95% Lower Boundary	CI-95% Upper Boundary	Random Factor Variation	CI-95% Lower Boundary	CI-95% Upper Boundary
--	-----------------------------	-----------------------------	-----------------------------	-------------------------------	-----------------------------	-----------------------------

Intercept (Ape Sclerae*Ape Skull)	0.1	-0.04	0.24	0.21	0.07	0.36
Human Sclerae	-0.1	0.29	0.09	0.19	0.04	0.41
Human Skull	-1.01	-1.33	-0.7	0.38	0.2	0.63
Human Sclerae*Human Skull	0.26	-0.16	0.66	0.37	0.16	0.64

Visual Exploration Patterns

Total Distance Travelled and Number of Visits

This study's hypotheses predict a negative effect of congruence on the number of visits and total distance travelled. To investigate the validity of these hypotheses, two multilevel models were computed. First, a negative binomial regression on the number of visits by skull and sclerae was run (see Table 3). The random participant effects of this model varied from 0.06 to 0.1, demonstrating relatively moderate differences in effects between participants. Second, a Gaussian regression was calculated to determine the effects of sclerae and skull on the total distance travelled (see Table 4). This model was used instead of a Gamma regression which could not be computed in R. Similar to the last model, variation between participants was estimated to be substantial, with estimates ranging from 52.13 to 61.93.

To properly interpret these models' results, it is relevant to note that effects of the negative binomial regression were multiplicative. This means that values above 1 indicate a

positive effect while those below 1 suggest a negative effect. Meanwhile, the Gaussian regression computed has additive effects, which means that values below 0 indicate negative effects while those above 0 suggest positive effects.

Both models show the same effect patterns (see Table 3 & 4). Namely, in comparison to fully ape-like stimuli, the effect sizes were consistently smaller for stimuli with one or both human features. This implies less visual exploration in response to faces with at least one human characteristic. Notably, this negative effect was the strongest for faces with human skulls and ape-like sclera. Additionally, the confidence interval for this effect predicts only negative effects, while those containing other combinations of human features also estimate possible positive effects. Therefore, reduced visual exploration was associated with human features, but especially with ape-like sclerae in human skulls.

Table 3

Multilevel Binomial Regression Coefficients of Number of Visits by Sclerae and Skull

	Fixed Effect Estimate	CI-95% Lower Boundary	CI-95% Upper Boundary	Random Effect	CI-95% Lower Boundary	CI-95% Upper Boundary
Intercept (Ape Sclerae*Ape Skull)	4.5	4.09	5.04	0.2	0.14	0.29
Human Sclerae	0.94	0.86	1.04	0.06	0.01	0.15
Human Skull	0.86	0.76	0.98	0.07	0.03	0.15

Human Sclerae*Human Skull	1.1	0.92	1.34	0.1	0.03	0.22
---------------------------	-----	------	------	-----	------	------

Table 4

Multilevel Gaussian Regression Coefficients of Total Distance Travelled by Sclerae and Skull

	Fixed Effect Estimate	CI-95% Lower Boundary	CI-95% Upper Boundary	Random Effect Estimate	CI-95% Lower Boundary	CI-95% Upper Boundary
Intercept (Ape Sclerae* Ape Skull)	386.20	296.41	478.32	212.52	158.22	284.56
Human Sclerae	-27.85	-91.34	32.68	59.30	12.97	119.98
Human Skull	-50.32	-133.78	32.02	52.13	18.71	104.58
Human Sclerae*Human Skull	59.26	-60.31	180.56	61.93	19.82	130.78

Dwell Time per AOI

In this study, it was hypothesised that areas other than the eyes are observed for longer amounts of time in response to incongruent faces relative to congruent faces. Due to the complexity and amount of data, it was not possible to run a multilevel analysis in *R*. To further simplify this analysis, the variables mouth and nose were merged into the variable snout. In Table 5, the multiplicative coefficients of a Gamma regression with sclerae and skull effects on dwell time per AOI are displayed. In Figure 6, combined effects are displayed.

Most notably, a conditional positive effect for eyes of congruent human faces was found, suggesting a longer dwell time on a fully human face's eyes. The second largest dwell times were predicted for fully ape-like stimuli, then faces with human sclerae in ape skulls, and lastly, human faces with ape-like sclerae (see Figure 6 & 7). As hypothesised, less time was spent looking at the eyes of incongruent faces. However, contrary to our hypotheses, these effects followed similar patterns for dwell time on the snout area.

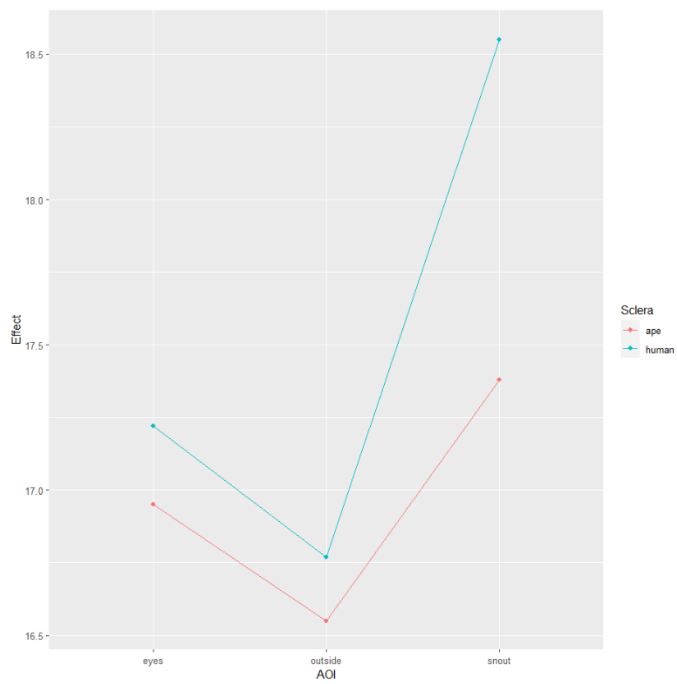
Table 5

Gamma Regression Coefficients of Dwell Time per AOI by Sclerae and Skull

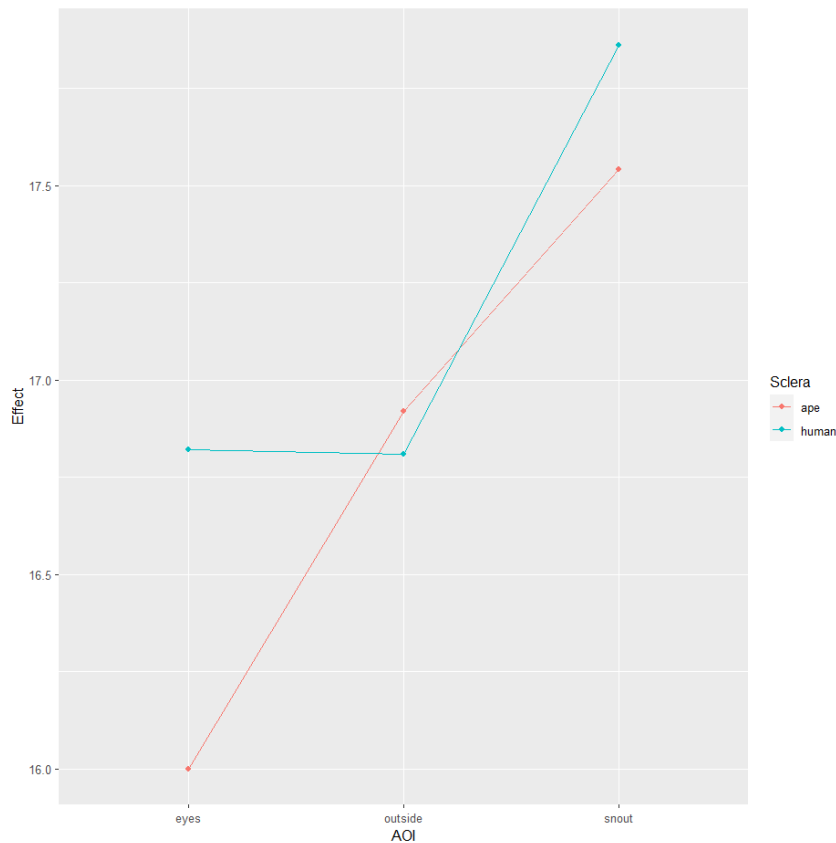
	Fixed Effect Estimate	CI-95% Lower Boundary	CI-95% Upper Boundary
Intercept (Eyes*Ape Sclerae*Ape Skull)	16.01	12.86	20.12
Outside	0.92	0.71	1.20
Snout	1.54	1.07	2.22
Human Sclerae	0.82	0.61	1.14
Human Skull	0.95	0.66	1.42
Outside*Human Sclerae	1.08	0.75	1.50
Snout*Human Sclera	1.47	0.89	2.32
Outside*Human Skull	0.63	0.41	0.94
Snout*Human Skull	0.92	0.50	1.62
Human Sclerae*Human Skull	1.57	1.14	2.16

Figure 6

Combined Effects of Sclera and Human Skull on Dwell Time per AOI

**Figure 7**

Combined Effects of Sclera and Ape Skull on Dwell Time per AOI



Discussion

To begin with, the hypothesis that incongruence between sclera colour and skull shape predicts that these faces are rated to be uncannier is true. This is in line with Kätsyri et al.'s (2015) mismatching feature hypothesis, which predicts that a mix of human-like and nonhuman features would be a determining factor in whether a face is perceived as uncanny. Furthermore, these results concur with Geue and Schmettow's (2021) finding that white sclerae on ape-like skulls contribute to lower likeability of faces. Contrary to this theory and our hypotheses, uncanniness ratings depended on the type of incongruence. That is, faces with ape-like sclerae and human skulls were rated as uncannier than faces with human sclerae and ape skulls. Similarly, visual exploration patterns supported the differences in effect strength of this type of incongruence. More specifically, there were fewer fixations and shorter distances travelled and less time spent on the eyes and snout of incongruent faces.

While these special effects on uncanniness ratings and eye movement behaviour for faces with ape-like sclerae and human skulls have not yet been discussed in scientific literature, these findings reflect design phenomena found in everyday life.

Dark Sclera on Human Faces in Video Games

Dark sclerae have been combined with human skulls in many types of entertainment media. For instance, this trope is used in video games to evoke a sense of horror, fear or discomfort in viewers. Popular examples of this include humanoid monsters in *The Witcher 3: Wild Hunt* (2015) and *The Elder Scrolls V: Skyrim* (2011). Meanwhile, there are numerous examples of animated animal-like characters with white sclerae which are portrayed as friendly. For instance, there are various creatures in the *Pokémon* franchise falling under this category. This phenomenon echoes our study's findings of a weaker effect for faces with white sclerae and ape-like skulls compared to faces with ape-like sclerae and human skulls. This calls the explanatory power of Kätsyri et al.'s (2015) perceptual mismatch hypothesis into question. Therefore, it could be useful to search for alternative explanations for the UVE.

Evolution and Dark Sclerae on Human Skulls

One possible explanation for why human skulls with dark sclera led to higher uncanniness ratings and effects on eye movement patterns may be rooted in the cooperative eye hypothesis (Tomasello et al., 2007; Kobayashi & Koshima, 2008). As a feature unique to humans, white sclera evolved for better communication among people (Kobayashi & Koshima, 2008). Hence, removing the readability of another human's gaze may seem especially uncooperative or even threatening. This untrustworthiness is likely enhanced as nonverbal communication is compromised, too. This is in line with Sabatelli and Rubin's

(1986) findings that showed that emotional expressivity is correlated with likeability, even independent of physical attractiveness.

Face Processing and Attention

A possible source of the eye movement patterns in response to incongruent stimuli may be found in cognitive face processing. That is, a lower number of fixation and total distance travelled may have been the result of holistic face processing, especially when confronted with faces with at least one or both human features (Mega & Volz, 2017). It is likely that a fully human skull with slight changes to sclera colour may have still triggered this type of face processing. Hence, it would be useful to take into account human likeness scores to compare eye movement patterns and UV scores in future research. However, this theory cannot solely explain why these effects were stronger for incongruent faces than congruent ones. Therefore, it is possible that uncanny, incongruent stimuli elicit calmer visual exploration responses than congruent faces.

This idea is somewhat supported by a study in the field of attentional research conducted by Horstmann (2015). More specifically, this scholar concluded that inconsistencies in sceneries lead to lower numbers of fixations (i.e., number of visits) on visually inconsistent objects. This was tested by using an image of a coherent environment that was changed to contain a surprising object at later stages of this researcher's trial. Unlike in Horstmann's (2015) study, however, fixation durations on eyes were smaller in incongruent conditions in our study.

A decreased dwell time on eyes and other central facial features is also opposite of the effect of what Cheetham et al.'s (2013) eye-tracking study on uncanny avatar faces and non-ambiguous human faces demonstrated. In their study, there were higher dwell times on the eyes and mouths of ambiguous avatar faces rather than on typical human faces. Further, there

were no actual differences in the number of fixations in response to more or less human-like stimuli. However, differences in the study's stimulus setup may have influenced these findings. Namely, Cheetham et al. (2013) 3D-modelled human-like avatars digitally. The researchers of this study did this by using photos of human faces that were then morphed to different degrees on a continuum, achieving faces varying in human likeness. The researchers confirmed this by running a forced categorisation pilot study. Meanwhile, in our study, photos of biological ape and human faces were used and then partially manipulated to have incongruent facial features (i.e., skull and sclera colour). On top of this, these incongruent faces were rated to be uncannier than those that were congruent. Therefore, stimuli selection differed in that Cheetham et al. (2013) utilised ambiguous faces with varying degrees of human likeness, while congruent and incongruent ape and human faces were used in our study. This could have had consequences for the types of face processing participants applied in these two studies, which may explain differences in eye-tracking data outcomes.

In overall visually ambiguous characters such as in Cheetham et al.'s (2013) study, these researchers found a dwell time shift from the nose to the eyes and mouth. This presumably happened as categorisation of ambiguous stimuli was more difficult due to small changes such as unrealistic shading affecting all parts of a face. Typically, the nose area serves as a key area in providing quick and broad spatial information, which aids in quick and broad face processing (Schyns et al., 2002; Schyns & McMurphy, 1994; Schyns & Olivia, 1994). Therefore, shifting attention away from this area to the nose and mouth may have indicated more detailed, and analytical processing of ambiguous faces. Meanwhile, incongruent stimuli used in our study contained merely one mismatching feature (i.e., sclera colour). Therefore, it may have been easier for participants to categorise the incongruent stimuli in our study. Based on this theory, it could have been useful to investigate how eye movement patterns may change over the course of looking at a clearly incongruent face. One

plausible reason for why participants' gazes wandered away from central features is that participants avoided feeling uncomfortable in response to uncanny stimuli. In brief, eye movement patterns appear to be influenced differently by different types of uncanniness.

The YET0-Eye Tracker

Notably, our study results show some first evidence of the feasibility of the *YET0-eye tracker* (Schmettow & Brandl, 2021). To minimise measurement error, future research should adhere to the following guidelines. First, to avoid glare from interfering with the software's eye identification, participants should remove their glasses. Secondly, similarly, the environment should be well-lit to ensure a sharp image. Third, a stable head mount should be made as the *YET0-eye tracker* does not track head movement. In practice, a pair of headphones or an empty glasses frame have proven relatively stable. Additionally, a headrest should be made for the participant so as to avoid head movements. Examples could include a full water bottle, a paper towel roll, a foam roller, and others. It would be advisable to design and 3D-print a chin rest for an even more stable and comfortable setup. Adhering to these guidelines, the results of our study were interpretable as the noise was reduced. However, there was bias due to low accuracy, which led to large confidence intervals. This bias may have been exacerbated by a relatively low sample size.

Despite this, the *YET0-eye tracker* may be useful for future research. That is, this eye tracker is less cost-intensive than other eye-tracking tools, allowing for it to be used in studies with low or no funding. Therefore, it would be beneficial to further test the *YET0-eye tracker's* accuracy and applicability in future studies. If proven useful, this tool could be used in student research. Possibly, larger samples could be collected as these cheap tools could be sent to participants' homes, especially during times in which social distancing is preferable.

Implications for Future Research

Using the *YETO-eye tracker* or similar eye-tracking devices in combination with our study's results, further studies could be conducted. To start off, this study was limited to static biological faces. However, in real-life designs of, for example, virtual avatars are typically animated and move. Tatler et al. (2011) have pointed out a similar problem for research on gaze behaviour in reaction to images of landscapes. It is plausible to assume that eye movement behaviours change in response to moving stimuli. In addition to this, bodily features other than faces may be relevant in the UVE, especially when there is a mismatch between face and body as it could lead to varying degrees of perceived human likeness. Additionally, this would be in line with Kätsyri et al.'s (2015) theory of the role of perceptual mismatch in the UVE.

However, the actual relevance of the perceptual mismatch hypothesis should be further investigated (Kätsyri et al., 2015). This could be done by using human likeness ratings to assess whether ape-like faces with human sclerae are viewed as more or less human-like. Then, likeability scores could be collected and related to these human likeness scores. The relationship between these scores and participants' eye movement patterns could be investigated.

Conclusion

In conclusion, this study's results show differences in eye movement patterns were influenced by types of incongruences of skull type and sclera colour. Most notably, the effect of dark ape-like sclerae on human skulls implies a stronger UVE effect for this condition. This could be explained by different face processing strategies and avoidance of unpleasant stimuli.

References

- Alvarez Perez, J., Garcia Goo, H., Sánchez Ramos, A., Contreras, V., & Strait, M. (2020). The Uncanny Valley manifests even with exposure to robots. *Companion of the 2020 ACM/IEEE International Conference on Human-Robot Interaction*, 101–103. <https://doi.org/10.1145/3371382.3378312>
- Avidan, G., Tanzer, M., & Behrmann, M. (2011). Impaired holistic processing in congenital prosopagnosia. *Neuropsychologia*, *49*(9), 2541–2552. <https://doi.org/10.1016/j.neuropsychologia.2011.05.002>
- Bagepally, B. S. (2015). Gaze pattern on spontaneous human face perception: An eye tracker study. *Journal of the Indian Academy of Applied Psychology*, *41*(3), 128-131.
- Bobrowsky, M. (2021, November 9). Big Tech Seeks Its Next Fortune in the Metaverse: From virtual-reality glasses to software to digital goods, emerging online realms promise new ways to make big bucks. *The Wall Street Journal*. <https://www.wsj.com/articles/big-tech-seeks-its-next-fortune-in-the-metaverse-11636459200>
- Burleigh, T. J., Schoenherr, J. R., & Lacroix, G. L. (2013). Does the uncanny valley exist? An empirical test of the relationship between eeriness and the human likeness of digitally created faces. *Computers in Human Behavior*, *29*(3), 759-771. <https://doi.org/10.1016/j.chb.2012.11.021>
- Cheetham, M., Suter, P., & Jäncke, L. (2011). The human likeness dimension of the “uncanny valley hypothesis”: Behavioral and functional MRI findings. *Frontiers in Human Neuroscience*, *5*(126), 126. <https://doi.org/10.3389/fnhum.2011.00126>
- Cheetham, M., Pavlovic, I., Jordan, N., Suter, P., & Jancke, L. (2013). Category processing and the human likeness dimension of the uncanny valley hypothesis: Eye-tracking data. *Frontiers in Psychology*, *4*(108). <https://doi.org/10.3389/fpsyg.2013.00108>

- Dahl, C. D., Rasch, M. J., & Chen, C. C. (2014). The other-race and other-species effects in face perception - A subordinate-level analysis. *Frontiers in Psychology, 5*(1068). <https://doi.org/10.3389/fpsyg.2014.01068>
- De Gelder, B., Meeren, H. K. M., Righart, R., van den Stock, J., van de Riet, W. A. C., & Tamietto, M. (2006). Chapter 3 Beyond the face: exploring rapid influences of context on face processing. *Visual Perception - Fundamentals of Awareness: Multi-Sensory Integration and High-Order Perception. Progress in Brain Research, 155*, 37–48. [https://doi.org/10.1016/s0079-6123\(06\)55003-4](https://doi.org/10.1016/s0079-6123(06)55003-4)
- De Haan, M., Humphreys, K., & Johnson, M. H. (2002). Developing a brain specialized for face perception: A converging methods approach. *Developmental Psychobiology, 40*(3), 200-212. <https://doi.org/10.1002/dev.10027>
- Di Giorgio, E., Méary, D., Pascalis, O., & Simion, F. (2013). The face perception system becomes species-specific at 3 months: An eye-tracking study. *International Journal of Behavioral Development, 37*(2), 95-99. <https://doi.org/10.1177/0165025412465362>
- Farah, M. J., Wilson, K. D., Drain, M., & Tanaka, J. N. (1998). What is "special" about face perception? *Psychological Review, 105*(3), 482–498. <https://doi.org/10.1037/0033-295X.105.3.482>
- Geue, L., & Schmettow, M. (2021). From robotics to primates: Tracing the uncanny valley effect to its evolutionary origin [Bachelor Thesis].
- Giuseppe, R., Mantivani, F., & Wiederhold, B. K. (2020). Positive Technology and COVID-19. *Cyberpsychology, Behavior, and Social Networking, 23*(9). <https://doi.org/10.1089/cyber.2020.29194.gri>
- Global Biodiversity Information Facility (n.d.). *Free and open access to biodiversity data*. <https://www.gbif.org/>
- Goren, C. C., Sarty, M., & Wu, P. Y. K. (1975). Visual following and pattern discrimination

of face-like stimuli by newborn infants. *Pediatrics*, 56(4), 544-549.

<https://doi.org/10.1542/peds.56.4.544>

Gurche, J. (n.d.). *John Gurche paleo artist*. Retrieved April 22, 2022, from

<https://gurche.com/>

Haeske, A. B., & Schmettow, M. (2016). The Uncanny Valley: Involvement of fast and slow evaluation systems. 49. [Bachelor's thesis, University of Twente].

<https://essay.utwente.nl/69091/>

Haxby, J., V., Hoffman, E. A., & Gobbini, M. I. (2000). The distributed human neural system for face perception. *Trends in Cognitive Sciences*, 4(6), 223-233.

[https://doi.org/10.1016/S1364-6613\(00\)01482-0](https://doi.org/10.1016/S1364-6613(00)01482-0)

Haxby, J. V., Hoffman, E. A., & Gobbini, M. I. (2002). Human neural systems for face recognition and social communication. *Biological Psychiatry*, 51(1), 59–67.

[https://doi.org/10.1016/S0006-3223\(01\)01330-0](https://doi.org/10.1016/S0006-3223(01)01330-0)

Ho, C.-C., & MacDorman, K. F. (2017). Measuring the uncanny valley effect: Refinements to indices for perceived humanness, attractiveness, and eeriness. *International Journal of Social Robotics*, 9(1), 129–139. <https://doi.org/10.1007/s12369-016-0380-9>

Hooge, I. T. C., Niehorster, D. C., Nyström, M., Andersson, R., & Hessels, R. S. (2022).

Fixation classification: How to merge and select fixation candidates. *Behavior Research Methods*. <https://doi.org/10.3758/s13428-021-01723-1>

Horstmann, G. (2015). The surprise-attention link: A review. *Annals of the New York Academy of Sciences*, 1339(1), 106-115. <https://doi.org/10.1111/nyas.12679>

Iskra, A., & Tomc, H. G. (2016). Eye-tracking analysis of face observing and face recognition. *Journal of Graphic Engineering and Design*, 7(1), 5-11.

<http://dx.doi.org/10.24867/JGED-2016-1-005>

Kaisler, R. E., & Leder, H. (2016). Trusting the looks of others: Gaze effects of faces in

- social setting. *Perception*, 45(8), 875-892. <https://doi.org/10.1177/0301006616643678>
- Kanwisher, N., & Yovel, G. (2006). The fusiform face area: A cortical region specialized for the perception of faces. *Philosophical Transactions of the Royal Society B*, 361(1476), <https://doi.org/10.1098/rstb.2006.1934>
- Kätsyri, J., Förger, K., Mäkäraänen, M., & Takala, T. (2015). A review of empirical evidence on different uncanny valley hypotheses: Support for perceptual mismatch as one road to the valley of eeriness. *Frontiers in Psychology*, 6(390), 1-16. <https://doi.org/10.3389/fpsyg.2015.00390>
- Kobayashi, H., & Kohshima, S. (1997). Unique morphology of the human eye. *Nature* 387, 767-768. <https://doi.org/10.1038/42842>
- Kobayashi, H., & Kohshima, S. (2001). Unique morphology of the human eye and its adaptive meaning: comparative studies on external morphology of the primate eye. *Journal of Human Evolution*, 40(5), 419-435. <https://doi.org/10.1006/jhev.2001.0468>
- Kobayashi, H., & Kohshima, S. (2008). Evolution of the human eye as a device for communication. In T. Matsuzawa (Ed.), *Primate origins of human cognition and behavior* (pp. 383-401). Springer. https://doi.org/10.1007/978-4-431-09423-4_19
- Landwehr, J. R., McGill, A. L., & Herrmann, A. (2011). It's Got the Look: The Effect of Friendly and Aggressive "Facial" Expressions on Product Liking and Sales. *Journal of Marketing*, 75(3), 132–146. <https://doi.org/10.1509/jmkg.75.3.132>
- Le Grand, R., Cooper, P. A., Mondloch, C. J., Lewis, T. L., Sagiv, N., de Gelder, B., & Maurer, D. (2006). What aspects of face processing are impaired in developmental prosopagnosia? *Brain and Cognition*, 61(2), 139–158. <https://doi.org/10.1016/j.bandc.2005.11.005>
- Le Grand, R., Mondloch, C. J., Maurer, D., & Brent, H. P. (2004). Impairment in holistic

- face processing following early visual deprivation. *Psychological Science*, *15*(11), 762–768. <https://doi.org/10.1111/j.0956-7976.2004.00753.x>
- MacDorman, K. F., Green, R. D., Ho, C.-C., & Koch, C.T. (2009). Too real for comfort? Uncanny responses to computer generated faces. *Computers in Human Behavior*, *25*(3), 695-710. <https://doi.org/10.1016/j.chb.2008.12.026>
- Marthur, M. B., & Reichling, D. B. (2016). Navigating a social world with robot partners: A quantitative cartography of the Uncanny Valley. *Cognition*, *146*, 22–32. <https://doi.org/10.1016/j.cognition.2015.09.008>
- Matsuda, Y.-T., Okamoto, Y., Ida, M., Okanoya, K., & Myowa-Yamakoshi, M. (2012). Infants prefer the faces of strangers or mothers to morphed faces: An uncanny valley between social novelty and familiarity. *Biology Letters*, *8*(5), 725–728. doi: 10.1098/rsbl.2012.0346
- McCarthy, G., Puce, A., Gore, J. C., & Allison, T. (1997). Face-specific processing in the human fusiform gyrus. *Journal of Cognitive Neuroscience*, *9*(5), 605-610. <https://doi.org/10.1162/jocn.1997.9.5.605>
- Mega, L. F., & Volz, K. G. (2017). Intuitive face judgments rely on holistic eye movement pattern. *Frontiers in Psychology*, *8*(1005). <https://doi.org/10.3389/fpsyg.2017.01005>
- Moore, R. K. (2012). A Bayesian explanation of the ‘Uncanny Valley’ effect and related psychological phenomena. *Scientific Reports*, *2*(864). <https://doi.org/10.1038/srep00864>
- Mori, M., MacDorman, K. F., & Kageki, N. (2012). The Uncanny Valley [From the Field]. *IEEE Robotics & Automation Magazine*, *19*(2), 98–100. <https://doi.org/10.1109/MRA.2012.2192811>
- Nowak, K. L., Hamilton, M. A., & Hammond, C. C. (2009). The effect of image features on

judgments of homophily, credibility, and intention to use as avatars in future interactions. *Media Psychology*, *12*(1), 50–76.

<https://doi.org/10.1080/15213260802669433>

Nowak, K. L., & Rauh, C. (2005). The influence of the avatar on online perceptions of anthropomorphism, androgyny, credibility, homophily, and attraction. *Journal of Computer-Mediated Communication*, *11*(1), 153–178. <https://doi.org/10.1111/j.1083-6101.2006.tb00308.x>

Nowak, K. L., & Rauh, C. (2008). Choose your “buddy icon” carefully: the influence of avatar androgyny, anthropomorphism and credibility in online interactions.

Computers in Human Behavior, *24*(4), 1473–1493.

<https://doi.org/10.1016/j.chb.2007.05.005>

RIKEN Center for Brain Science (2018). *PrimFace: Face database of non-human primates*. <https://visiome.neuroinf.jp/primface/>

Provine, R. R., Cabrera, M. O., & Nave-Blodgett, J. (2013). Red, yellow, and super-white sclerae uniquely human cues for healthiness, attractiveness, and age. *Human Nature*, *24*(2), 126–137. <https://doi.org/10.1007/s12110-013-9168-x>

Reips, U.-D., & Funke, F. (2008). Interval-level measurement with visual analogue scales in Internet-based research: VAS generator. *Behavior Research Methods*, *40*(3), 699–704.

<https://doi.org/10.3758/BRM.40.3.699>

Richler, J. J., & Gauthier, I. (2014). A meta-analysis and review of holistic face processing. *Psychological Bulletin*, *140*(5), 1281–1302. <https://doi.org/10.1037/a0037004>

Rosch, E., Mervis, C. B., Gray, W. D., Johnson, D. M., & Boyes-Braem,

P. (1976). Basic objects in natural categories. *Cognitive Psychology*, *8*(3), 382–439.

[https://doi.org/10.1016/0010-0285\(76\)90013-X](https://doi.org/10.1016/0010-0285(76)90013-X)

Sabatelli, R. M., & Rubin, M. (1986). Nonverbal expressiveness and physical attractiveness

- as mediators of interpersonal perceptions. *Journal of Nonverbal Behavior*, *10*, 120-133. <https://doi.org/10.1007/BF01000008>
- Salvucci, D. D., & Goldberg, J. H. (2000). *Identifying fixations and saccades in eye-tracking protocols*. In Proceedings of the Eye Tracking Research and Applications Symposium (pp. 71-78). New York: ACM Press.
- Santos, I. M., & Young, A. W. (2011). Inferring social attributes from different face regions: Evidence for holistic processing. *Quarterly Journal of Experimental Psychology*, *64*(4), 751-766. <https://doi.org/10.1080/17470218.2010.519779>
- Schmettow, M., & Brandl, L. (2021, November 2). *Programming for Psychologists: A first course in Python*. https://schmettow.github.io/PfP_Book/intro.html#batchwork
- Schmettow, M. (2021, December 23). *New statistics for design researchers: A Bayesian workflow in tidy R*. https://schmettow.github.io/New_Stats/index.html#whom-for
- Schyns, P. G., Bonnar, L., & Gosselin, F. (2002). Show me the features! Understanding recognition from the use of visual information. *Psychological Science*, *13*(5), 402-409. <https://doi.org/10.1111/1467-9280.00472>
- Schyns, P. G., & Murphy, G. (1994). *The ontogeny of part representation in object concepts*. (Institute Cognitive Science Technical Report #CS91-14). Beckman Institute.
- Schyns, P. G., & Oliva, A. (1994). From blobs to boundary edges: Evidence for time- and spatial-scale-dependent scene recognition. *Psychological Science*, *5*(4), 195-200. <https://doi.org/10.1111/j.1467-9280.1994.tb00500.x>
- Shin, M., Song, S. W., & Chock, T. M. (2019). Uncanny Valley Effects on friendship decisions in virtual social networking service. *Cyberpsychology, Behavior, and Social Networking*, *22*(11), 700-705. <https://doi.org/10.1089/cyber.2019.0122>
- Starmans, C., & Bloom, P. (2012). Windows to the soul: Children and adults see the eyes as

- the location of the self. *Cognition*, *123*(2), 313-318.
<https://doi.org/10.1016/j.cognition.2012.02.002>
- Steckenfinger, S. A., & Ghazanfar, A. A. (2009). Monkey visual behavior falls into the uncanny valley. *Proceedings of the National Academy of Sciences*, *106*(43), 18362–18366. <https://doi.org/10.1073/pnas.0910063106>
- Tanaka, J. W., & Farah, M. J. (1993). Parts and wholes in face recognition. *The Quarterly Journal of Experimental Psychology Section A*, *46*(2), 225–245.
<https://doi.org/10.1080/14640749308401045>
- Tanaka, J. W., & Sung, A. (2013). The “Eye Avoidance” Hypothesis of autism face processing. *Journal of Autism and Developmental Disorders*, *46*, 1538-1552.
<https://doi.org/10.1007/s10803-013-1976-7>
- Tatler, B. W., Hayhoe, M. M., Land, M. F., & Ballard, D. H. (2011). Eye guidance in natural vision: Reinterpreting salience. *Journal of Vision*, *11*(5).
<https://doi.org/10.1167/11.5.5>
- The Elder Scrolls V: Skyrim. [Computer Software]. (2011). Bethesda Game Studios.
- The Witcher 3: Wild Hunt. [Computer Software]. (2015). CD Projekt Red.
- Todorov, A., Baron, S. G., & Oosterhof, N. N. (2008). Evaluating face trustworthiness: A model based approach. *Social Cognitive and Affective Neuroscience*, *3*(2), 119–127.
<https://doi.org/10.1093/scan/nsn009>
- Tomasello, M., Hare, B., Lehmann, H., & Call, J. (2007). Reliance on head versus eyes in the gaze following of great apes and human infants: the cooperative eye hypothesis. *Journal of Human Evolution*, *52*(3), 314–320.
<https://doi.org/10.1016/j.jhevol.2006.10.001>
- Urgen, B. A., Kutas, M., & Saygin, A. P. (2018). Uncanny valley as a window into predictive

processing in the social brain. *Neuropsychologia*, *114*, 181-185.

<https://doi.org/10.1016/j.neuropsychologia.2018.04.027>

Valenza, E., Simion, F., Cassia, V. M., & Umiltà, C. (1996). Face preference at birth. *Journal of Experimental Psychology: Human Perception and Performance*, *22*(4), 892–903.

<https://doi.org/10.1037/0096-1523.22.4.892>

Walther, J. B., & Bunz, U. (2005). The rules of virtual groups: Trust, liking, and performance in computer-mediated communication. *Journal of Communication*, *55*(4), 828–846.

<https://doi.org/10.1111/j.1460-2466.2005.tb03025.x>

Wiederhold, B. K. (2022). Ready (or Not) Player One: Initial musings on the Metaverse.

Cyberpsychology, Behavior, and Social Networking, *25*(1).

<https://doi.org/10.1089/cyber.2021.29234.editorial>

Young, A. W., Hallowell, D., & Hay, D. C. (1987). Configurational information in face perception. *Perception*, *16*(11), 747–759. <https://doi.org/10.1068/p160747>

Yu, N. (2001). What Does Our Face Mean to Us? *Pragmatics & Cognition*, *9*, 1–36.

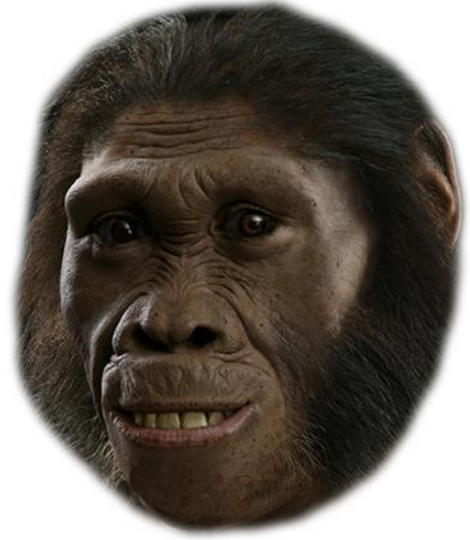
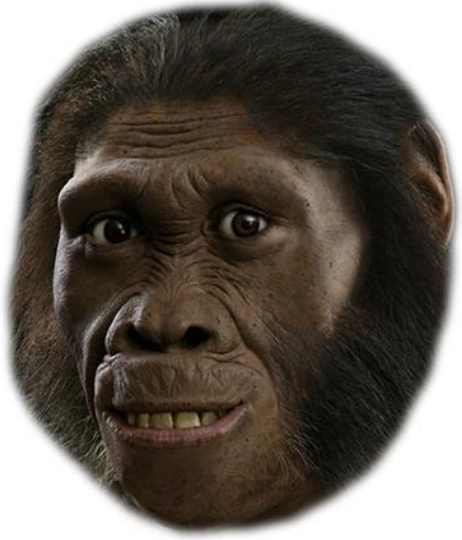
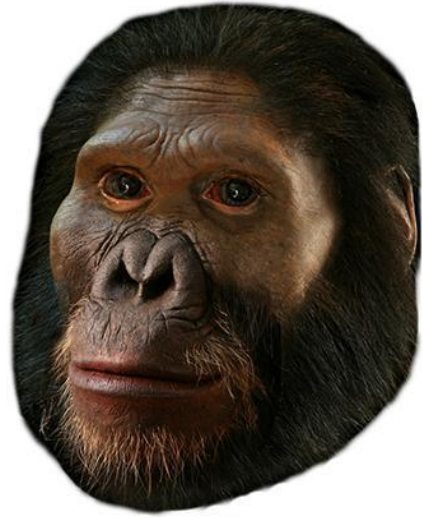
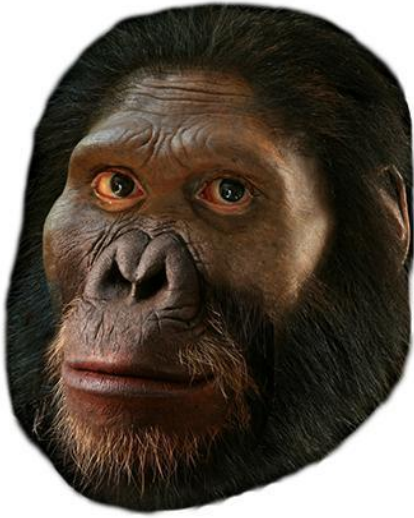
<https://doi.org/10.1075/pc.9.1.02yu>

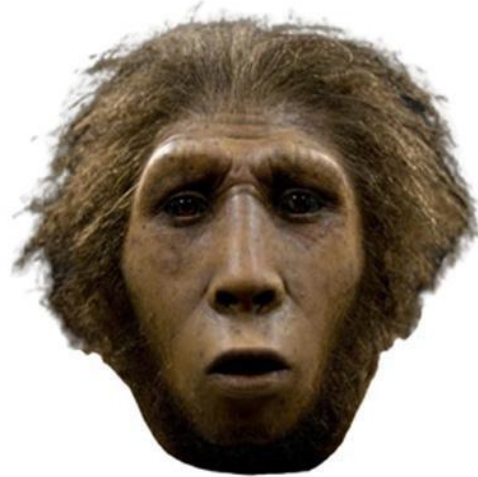
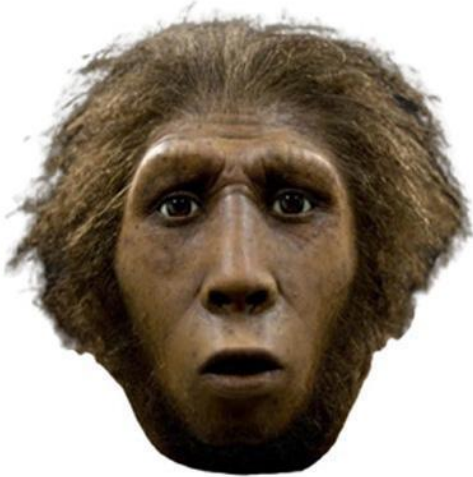
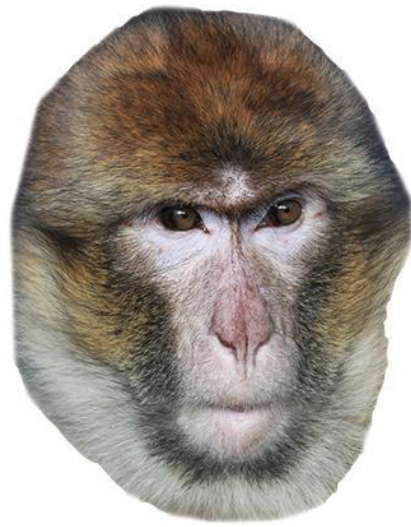
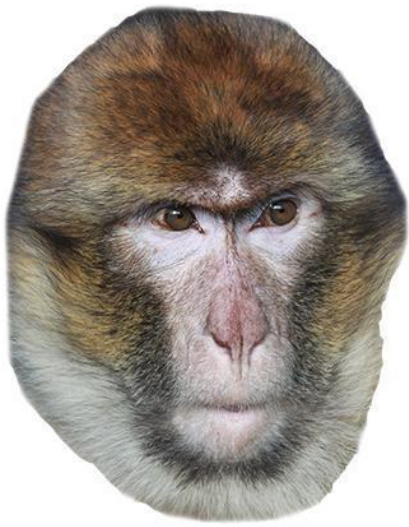
Appendix A: Stimulus Set

Original

Manipulated







Appendix B: Participant Forms

Information Sheet

The Significance of Sclera Colour in the Uncanny Valley Effect: An Eye Tracking Study

Purpose

The Uncanny Valley Effect describes a drop in how likable a face (or character) is at a moderate-to-high human likeness. Therefore, people may feel slight discomfort or eeriness in response to faces (or characters) that have some human features mixed in with some non-human features. This study seeks to examine the significance of the eyes and general differences in visual exploration patterns in the Uncanny Valley Effect. For this, you will be asked to rate how uncanny you find faces presented to you while your eyes will be video-recorded to gather eye-tracking data. The study will take approximately 15 minutes to complete.

This study has been approved by the BMS Ethics Committee.

Risks

In response to looking at uncanny faces, you may feel a slight discomfort which is why we have limited exposure to a minimum.

Right to Withdrawal

You have the right to withdraw from this study at any given time without any particular reason.

Anonymisation of data

Any of your personal information will be immediately anonymized for further data analysis purposes. Any of your personal information (e.g., your name) will be handled confidentially by the three researchers of this study (see at the bottom of this sheet).

Data Usage

We will video record your eyes which will be translated into eye-tracking data in the form of coordinates. These will be used to analyse how much distance your eyes travel in total, how often you look from one facial feature to another, and on which facial features you focus the most. This is so that we can investigate whether you visually explore faces differently depending on how uncanny they are to you. The degree of uncanniness will be determined based on your rating scale data.

Any video footage will be immediately destroyed after you complete, or withdraw from, this study. The anonymised data will be shared between the three researchers (see at the bottom of this sheet) and their supervisors. In accordance with APA (American Psychological Association) guidelines, this data will be stored for five years, upon which it will be destroyed. The anonymised data will be used as part of a Bachelor thesis research report, which will be published in the University of Twente's online repository.

For further information (e.g., on study results), please contact:

Jamy L. M. Borninkhof: j.l.m.borninkhof@student.utwente.nl

Marc G. van Dijk: m.g.vandijk@student.utwente.nl

Isa Dollée: i.dollee@student.utwente.nl

Contact Information for Questions about Your Rights as a Research Participant: If you have questions about your rights as a research participant, or wish to obtain information, ask questions, or discuss any concerns about this study with someone other than the researcher(s), please contact the Secretary of the Ethics Committee/domain Humanities & Social Sciences of the Faculty of Behavioural, Management and Social Sciences at the University of Twente by ethicscommittee.hss@utwente.nl

UNIVERSITY OF TWENTE.

Informed Consent Form

The Significance of Sclera Colour in the Uncanny Valley Effect: An Eye-Tracking Study

Please tick the appropriate boxes

Yes

Taking part in the study

I have read and understood the study information, or it has been read to me. I have been able to ask questions about the study and my questions have been answered to my satisfaction.

I consent voluntarily to be a participant in this study and understand that I can refuse to answer questions and I can withdraw from the study at any time, without having to give a reason.

I understand that taking part in the study involves the recording of my eyes in video-only form and, therefore, the recording of my eye-tracking data. The only data that will be kept is eye-tracking data, which encompasses coordinates indicating how my eyes move and focus on the pictures presented to me. Any video footage will be immediately destroyed. Further, this study involves the ratings I fill in on the rating scales provided to me in print form.

Risks associated with participating in the study

I understand that taking part in the study involves the following risks:

Slight discomfort in response to presentation of uncanny faces.

Use of the information in the study

I understand that the anonymous information I provide will be used for the three researchers' Bachelor theses research reports, which may be published on the University of Twente's online repository.

I understand that personal information collected about me that can identify me, such as [e.g., my name or where I live], will not be shared beyond the study team.

Consent to be video recorded

I agree be video recorded.

Signatures_____
Name of participant_____
Signature_____
Date

I have accurately read out the information sheet to the potential participant and, to the best of my ability, ensured that the participant understands to what they are freely consenting.

Researcher name_____
Signature_____
Date**For further information, contact:***Jamy L. M. Borninkhof: j.l.m.borninkhof@student.utwente.nl**Marc G. van Dijk: m.g.vandijk@student.utwente.nl**Isa Dollée: i.dollee@student.utwente.nl***Contact Information for Questions about Your Rights as a Research Participant:**

If you have questions about your rights as a research participant, or wish to obtain information, ask questions, or discuss any concerns about this study with someone other than the researcher(s), please contact the Secretary of the Ethics Committee/domain Humanities & Social Sciences of the Faculty of Behavioural, Management and Social Sciences at the University of Twente by ethicscommittee-hss@utwente.nl

UNIVERSITY OF TWENTE.

Appendix C: R Code

```

---
title: "YET with R basic workflow"
author: "M Schmettow"
date: "09/05/2022"
output: html_document
---

```{r setup, include=FALSE}
knitr::opts_chunk$set(echo = TRUE)
knitr::opts_chunk$set(fig.width = 8)
knitr::opts_chunk$set(fig.height = 8)
data_path = "CSV"
```

```{r}
library(tidyverse)
library(printr)

require(readxl)
require(jpeg)
require(ggimg)
```

# Preparation

```{r}
WIDTH = 450
HEIGHT = 450
IMG_DIR = "Images/"
```

## Reading csv

```{r}
csv_files <- dir(path = data_path,
 pattern = "*.csv",
 recursive = T,
 full.names = T)

UV22_0 <-
 csv_files %>%
 map_df(~read_csv(.x,
 col_types = cols(Part = col_double()), # <-- we change this later

```

```

Obs = col_double(),
 time = col_double(),
 x = col_double(),
 y = col_double(),
 Picture = col_character()
)) %>%
 mutate(File = .x) %>%
 mutate(is_duplicate = lag(x) == x & lag(y) == y) %>% ## Yeta1 seems to duplicate
measures. This is a bugfix
 filter(!is_duplicate) %>%
 filter(!str_detect(Picture, "dummy")) %>%
 mutate(Obs = row_number()) %>%
 mutate(Part = as.factor(as.integer(Part - min(Part)) + 1)) %>% ## reducing the Part
identifier
 group_by(Part) %>%
 mutate(time = time - min(time)) %>% # time since start experiment
 ungroup() %>%
 mutate(y = HEIGHT - y, #### reversing the y-axis
 manipulated = stringr::str_detect(Picture, "manipulated"),
 Face = stringr::str_extract(Picture, "[0-9]+"),
 humlike = as.numeric(Face)) %>%
 select(Obs, Part, Picture, Face, humlike, manipulated, time, x, y)

sample_n(UV22_0, 10)

summary(UV22_0, 10)
```



### ## Reading PictureInfo and AOI



```

```{r}
Pinfo <-
  read_csv(str_c(IMG_DIR, "PictureInfo.csv"),
           col_types = cols(File = col_character(),
                            width = col_double(),
                            height = col_double(),
                            humLike = col_double(),
                            humskull = col_logical(),
                            whitesclera = col_logical(),
                            congruency = col_double())
  )) %>%
  rename(Picture = File) %>%
  mutate(Skull = if_else( humskull, "human", "ape"),

```


```

```

Sclera = if_else(whitesclera, "human", "ape"),
congruent = (Sclera == Skull))

UV22_1 <- left_join(UV22_0, Pinfo,
 by = "Picture") %>%
 select(Obs, Part, Picture, Face, humlike, Sclera, Skull, congruent, time, x, y)
...

```{r}
AOI <-
  readxl::read_xlsx("AOI.xlsx") %>%
  #right_join(Pinfo, by = "Picture") %>%
  mutate(Face = str_extract(Picture, "[0-9]+"),
    Path = str_c(IMG_DIR, Picture, sep = ""),
    #Image = map(Path, ~jpeg::readJPEG(.x)),
    xmin = x,
    xmax = x + w,
    ymax = HEIGHT - y, ## reversing the y coordinates
    ymin = HEIGHT - (y + h)) %>%
  arrange(Face, AOI) %>%
  select(Face, AOI, xmin, xmax, ymin, ymax, Path)

head(AOI)
...

## Data preparation

- measuring distance and duration
- vertical mirroring off coordinates
- extracting variables from file names
- shortening some variables

```{r}
UV22_2 <-
 UV22_1 %>%
 mutate(Sequence = as.factor(str_c(Part, Picture, sep = "_"))) %>%
 group_by(Sequence) %>%
 mutate(distance = sqrt((x - lag(x))^2 + ## Euclidian distance
 (y - lag(y))^2),
 duration = lead(time) - time) %>% ## duration
 ungroup() %>%

```

```

 select(Obs, Part, Picture, Face, Sequence, humlike, Sclera, Skull, congruent, time, x, y,
distance, duration) %>%
 filter(Face != "dummy")

```

```

sample_n(UV22_2, 10)

```

```

summary(UV22_2)
```

```

```

# Visualization

```

```

## Grid of pictures

```

We create a re-usable ggplot object G_0 containing a grid of pictures

```

```{r, fig.height = 8, fig.width = 8}
G_0 <-
 AOI %>%
 ggplot(aes(xmin = xmin, xmax = xmax, ymin = ymin, ymax = ymax)) +
 facet_wrap(~Face) +
 ggimg::geom_rect_img(aes(img = Path, xmin = 0, xmax = WIDTH, ymin = 0, ymax =
HEIGHT)) +
 xlim(0, WIDTH) +
 ylim(0, HEIGHT)

```

```

G_0
```

```

```

## Raw measures visualization

```

```

```{r}
G_0 +
 geom_point(aes(x = x, y = y, col = Part),
 size = .5,
 alpha = .5,
 inherit.aes = F,
 data = UV22_2)
```

```

```

## AOI visualization

```

```

```{r fig.height = 8, fig.width = 8}

```

```

G_1 <-
 G_0 +
 geom_rect(aes(xmin = xmin, ymin = ymin,
 xmax = xmax, ymax = ymax,
 fill = AOI),
 alpha = .2,
 inherit.aes = F)

G_1
```



```

AOI Classification

```{r}
UV22_3 <-
  UV22_2 %>%
  left_join(AOI, by = "Face") %>%
  mutate(is_in = x > xmin & x < xmax & y > ymin & y < ymax) %>%
  filter(is_in) %>%
  select(Obs, AOI) %>%
  right_join(UV22_2, by = "Obs") %>%
  mutate(AOI = if_else(is.na(AOI), "Outside", AOI)) %>%
  arrange(Part, time)

summary(UV22_3)
```

```{r}
UV22_3 %>%
  group_by(AOI) %>%
  summarize(n())

```

```{r}
G_0 +
  geom_point(aes(x = x, y = y,
                col = AOI),
            size = .5,
            alpha = .5,
            inherit.aes = F,
            data = UV22_3)
```

```


```

```

```{r}
G_0 +
 geom_count(aes(x = x, y = y,
 col = AOI),
 alpha = .5,
 inherit.aes = F,
 data = UV22_3)
```

```

Measuring visits

A *visit* is a closed sequence of eye positions in the same region. The following code uses a combined criterion for setting new visits:

- the position falls into a different AOI
- OR: the distance traveled from the previous position exceeds a certain threshold

```

```{r}
distance_threshold <- 50

UV22_4 <-
 UV22_3 %>%
 group_by(Part, Picture) %>%
 filter(AOI != lag(AOI) | distance > distance_threshold) %>% ## logical OR
 mutate(visit = row_number(),
 duration = lead(time) - time) %>%
 ungroup()

sample_n(UV22_4, 10)
```

```

Plotting visit paths and duration

```

```{r fig.width=8, fig.height = 8}
G_3 <-
 G_0 +
 geom_point(aes(x = x, y = y,
 shape = Part,
 size = duration), # <--
 alpha = .5,
 inherit.aes = F,
 data = UV22_4)
```

```

```
G_3
```
```

```
```{r}
```

```
G_4 <-
  G_0 +
  geom_path(aes(x = x, y = y,
                col = Part),
            inherit.aes = F,
            data = UV22_4) # <--
```

```
G_4
```
```

```
Population-level AOI frequencies
```

```
```{r}
```

```
UV22_5 <-
  UV22_4 %>%
  group_by(AOI, congruent, Face, Part) %>%
  summarize(n_visits = n(),
            total_dur = sum(duration, na.rm = TRUE)) %>%
  ungroup()
```

```
UV22_5
```
```

```
```{r}
```

```
G_5 <-
  UV22_5 %>%
  ggplot(aes(x = AOI, y = n_visits, fill = congruent)) +
  geom_col()
```

```
G_5
```
```

```
Frequencies per participant
```

```
```{r}
```

```
UV22_6 <-
  UV22_4 %>%
  group_by(Part, Face, AOI, congruent, Sclera, Skull) %>% # <--
  summarize(n_visits = n(),
            total_dur = sum(duration, na.rm = TRUE)) %>%
  ungroup()
```



```
sample_n(UV22_6, 10)
```

```

```
```{r}
G_6 <-
  UV22_6 %>%
  ggplot(aes(x = congruent, y = n_visits, fill = AOI)) +
  facet_wrap(~Part) +
  geom_col()

```

```
G_6
```

```

```
Durations per participant
```

```
```{r}
G_7 <-
  UV22_6 %>%
  ggplot(aes(x = AOI, y = total_dur, fill = manipulated)) +
  facet_wrap(~Part) +
  geom_col()

```

```
G_6
```

```

```
```{r}
save(AOI, UV22_1, UV22_2, UV22_3, UV22_4, UV22_5, UV22_6, file = "UV22.Rda")
```

```

```
Your analysis
```

```
Reading the ratings
```

```
```{r}
UV22_7 <-
  read_xlsx("Ratings of Uncanniness .xlsx") %>%
  pivot_longer(-Part,
               names_to = "Picture",
               values_to = "rating") %>%
  left_join(Pinfo) %>%
  select(Part, Picture, humLike, congruency, Skull, Sclera, rating)

```

```
```
```

```
```{r}
load(file = "UV22.Rda")
```
```

```
```{r}
library(rstanarm)
options(mc.cores = 4)
library(bayr)
```
```

Preparing data sets

Filtering out incorrectly manipulated picture

```
```{r}
sample_n(UV22_4, 3)
```

```
UV22_4 <- UV22_4 %>%
  filter(Face != "27")
```

```
UV22_4$pos_curve <- cut(UV22_4$humble,
  breaks=c(0, 50, 80, 100),
  labels=c('shoulder', 'valley', 'upwards slope'))
```

```
sample_n(UV22_4, 3)
```
```

```
```{r}
UV22_5 <- UV22_5 %>%
  filter(Face != "27")
sample_n(UV22_5, 10)
```

```
UV22_6 <- UV22_6 %>%
  filter(Face != "27")
sample_n(UV22_6, 10)
```
```

Computing outcome variables

```
```{r}
UV22_8 <-
  UV22_4 %>%
  filter(congruent != "NA") %>%
```



```

...

```{r}
fixef(M_rating2)
```

##### graph by congruence
```{r}
G_rating <-
 UV22_7 %>%
 ggplot(aes(x = congruency, y = rating_final)) +
 geom_col()

G_rating
```

##### by congruence, multi-level
```{r}
M_rating3 <- stan_glmer(rating_final ~ 1 + congruency + (1 + congruency | Part),
 data = UV22_7,
 family=mgcv::betar(link = "logit"))
```

```{r}
fixef(M_rating3) #fixed effects
grpgef(M_rating3) #random effects
```

##### by sclera and skull, multi level
```{r}
M_rating4 <- stan_glmer(rating_final ~ 1 + Sclera * Skull + (1 + Sclera * Skull | Part),
 data = UV22_7,
 family=mgcv::betar(link = "logit"))
```

```{r}
fixef(M_rating4) #fixed effects
grpgef(M_rating4) #random effects
```

#### H2: N_visits

##### by congruence, population level
```{r}

```

```

M_3 <- stan_glm(n_visits ~ 1 + congruent,
 data = UV22_5,
 family = neg_binomial_2())
...

```{r}
fixef(M_3, mean.func = exp)
...

##### by sclera and skull, population level
```{r}
M_4 <- stan_glm(n_visits ~ 1 + Sclera * Skull,
 data = UV22_6,
 family = neg_binomial_2())
...

```{r}
fixef(M_4, mean.func = exp)
...

##### could be used for graph by sclera and skull
```{r}
M_5 <- stan_glm(n_visits ~ 0 + Sclera : Skull,
 data = UV22_6,
 family = neg_binomial_2())
...

```{r}
fixef(M_5, mean.func = exp)
...

##### graph by congruence
```{r}
G_visits <-
 UV22_5 %>%
 ggplot(aes(x = congruent, y = n_visits)) +
 geom_col()

G_visits
...

by congruence, multi-level
```{r}
M_visits1 <- stan_glmer(n_visits ~ 1 + congruent + (1 + congruent | Part),

```

```

    data = UV22_5,
    family = neg_binomial_2()
  ...

  ```{r}
 fixef(M_visits1, mean.func = exp) #fixed effects
 grpuf(M_visits1, mean.func = exp) #random effects
 ...

 ##### by sclera and skull, multi level
  ```{r}
  M_visits2 <- stan_glmer(n_visits ~ 1 + Sclera * Skull + (1 + Sclera * Skull | Part),
    data = UV22_6,
    family = neg_binomial_2())
  ...

  ```{r}
 fixef(M_visits2, mean.func = exp) #fixed effects
 grpuf(M_visits2, mean.func = exp) #random effects
 ...

 ### H2: Total distance travelled
 ##### by congruence, population level
  ```{r}
  M_dist1 <- stan_glm(total_dist ~ 1 + congruent,
    data = UV22_8,
    family = Gamma())
  ...

  ```{r}
 fixef(M_dist1, mean.func = exp)
 ...

 ##### by sclera and skull, population level
  ```{r}
  M_dist2 <- stan_glm(total_dist ~ 1 + Sclera * Skull,
    data = UV22_8,
    family = Gamma())
  ...

  ```{r}

```

```

fixef(M_dist2, mean.func = exp)
```

#### graph by congruence
```{r}
G_dist <-
 UV22_8 %>%
 ggplot(aes(x = congruent, y = total_dist)) +
 geom_col()

G_dist
```

####by sclera and skull, multi level
```{r}
MLM_dist2 <- stan_glmer(total_dist ~ 1 + Sclera * Skull + (1 + Sclera * Skull | Part),
 data = UV22_8,
 family = gaussian)
```

```{r}
fixef(MLM_dist2) #fixed effects
grpef(MLM_dist2) #random effects
```

### H3: AOI

```{r}
UV22_4 %>%
 group_by(AOI, congruent) %>%
 summarize(mean_dur = mean(duration, na.rm = TRUE),
 sd_dur = sd(duration, na.rm = TRUE))
```

#### by congruence, population level
```{r}
M_1 <-
 UV22_4 %>%
 stan_glm(duration ~ 1 + AOI + congruent + AOI:congruent, # AOI*congruence
 data = .,
 family = Gamma())
```

```

```

```{r}
fixef(M_1)
```

#### by congruence, population level, for graph
```{r}
M_2 <-
 UV22_4 %>%
 stan_glm(duration ~ 0 + AOI:congruent,
 data = .)

```

```{r}
fixef(M_2)
```

```{r}
T_2 <-
 fixef(M_2) %>%
 mutate(fixef = str_remove_all(fixef, "AOI|congruent")) %>%
 separate(fixef, into = c("AOI", "congruence")) %>%
 select(AOI, congruence, center, lower, upper)

T_2
```

```{r}
T_2 %>%
 ggplot(aes(x = AOI, col = congruence,
 y = center, ymin = lower, ymax = upper)) +
 geom_point() +
 geom_line(aes(group = congruence))
```

#### by sclera and skull, population level
```{r}
M_AOI_1 <- UV22_4 %>%
 stan_glm(duration ~ 1 + AOI + Sclera + Skull + AOI:Sclera + AOI:Skull + Sclera:Skull,
 data = .,
 family = Gamma())
```

```



```

```{r}
fixef(M_AOI_1, mean.func = exp)
```

##### by congruence, multi-level
```{r}
MLM_AOI1 <- stan_glmer(duration ~ 1 + AOI + congruent + AOI:congruent (1 + AOI +
congruent + AOI:congruent | Part),
data = UV22_4,
family = Gamma())
```

```{r}
fixef(MLM_AOI1, mean.func = exp) #fixed effects
grpuf(MLM_AOI1, mean.func = exp) #random effects
```

##### by sclera and skull, multi level
```{r}
MLM_AOI2 <- stan_glmer(duration ~ 1 + AOI + Sclera + Skull + AOI:Sclera + AOI:Skull +
Sclera :Skull + (1 + AOI + Sclera + Skull + AOI:Sclera + AOI:Skull + Sclera:Skull | Part),
data = UV22_4,
family = Gamma())
```

```{r}
fixef(MLM_AOI2, mean.func = exp) #fixed effects
grpuf(MLM_AOI2, mean.func = exp) #random effects
```

#####Graph
```{r}
AOI <- c("eyes", "eyes", "eyes", "eyes",
 "outside", "outside", "outside", "outside",
 "snout", "snout", "snout", "snout")
Sclera <- c("ape", "human", "ape", "human",
 "ape", "human", "ape", "human",
 "ape", "human", "ape", "human")
Skull <- c("ape", "ape", "human", "human",
 "ape", "ape", "human", "human",
 "ape", "ape", "human", "human")
Effect <- c(16, 16.82, 16.95, 17.22,
 16.92, 16.81, 16.55, 16.77,

```

17.54, 17.86, 17.38, 18.55)

```
T_graph <- data.frame(AOI, Sclera, Skull, Effect)
```

```
T_graph
```

```
```\n
```

```
```\n{r}
```

```
T_graph %>%
 filter(Skull == "human") %>%
 ggplot(aes(x = AOI, col = Sclera, y = Effect)) +
 geom_point() +
 geom_line(aes(group = Sclera))
```

```
T_graph %>%
 filter(Skull == "ape") %>%
 ggplot(aes(x = AOI, col = Sclera, y = Effect)) +
 geom_point() +
 geom_line(aes(group = Sclera))
```\n
```